Journal of Asian Earth Sciences 273 (2024) 106254

Contents lists available at ScienceDirect

Journal of Asian Earth Sciences

journal homepage: www.elsevier.com/locate/jseaes

Mesozoic tectonic evolution and dynamic mechanisms of the northern Bozhong depression of the Bohai Bay Basin, eastern China

Fan Yang [a,b], Yixin Yu [a,b,*], Xintao Zhang [c], Yuhang Chen [d], Yongjun Liu [e], Zhen Zhang [e], Peng Qi [f], Yuemeng Niu [a,b]

[a] National Key Laboratory of Petroleum Resources and Engineering, China University of Petroleum (Beijing), Beijing 102249, China
[b] College of Geosciences, China University of Petroleum (Beijing), Beijing 102249, China
[c] Exploration and Development Department of CNOOC Limited, Beijing 100010, China
[d] Research Institute of Exploration and Development, PetroChina Changqing Oilfield Company, Xi'an 710018, China
[e] Tianjin Branch of CNOOC (China), Tianjin 300459, China
[f] CNOOC Research Institute Company Limited, Beijing 100028, China

ARTICLE INFO

Keywords:
Fault
Tectonic evolution
Dynamic mechanisms
Mesozoic
Northern Bozhong depression
Bohai Bay Basin

ABSTRACT

The northern Bozhong depression of the Bohai Bay Basin in eastern China is an important area for oil and gas exploration in buried hills, which has complex structural styles and evolutionary processes. Based on 3D seismic and drilling data, the features of the Mesozoic structural deformation of the northern Bozhong depression are analyzed, and the tectonic evolution and dynamic mechanisms are also discussed. The complex Mesozoic structural styles of the northern Bozhong depression are composed of compression, strike-slip, and extension structures, which mainly trend in the near E-W, NW, NE, and NNE directions. Triggered by the collision and subduction between the North China, South China and Izanagi plates and associated stress fields of different periods, natures and directions, the northern Bozhong depression has experienced five stages of deformation at the end of the Middle Triassic, the Late Triassic, the Early-Middle Jurassic, the Late Jurassic-Early Cretaceous and the Late Cretaceous. Cyclical tectonic evolution has controlled the development of structural styles of different strikes and natures and the spatial distribution of strata in the northern Bozhong depression, providing an important foundation for hydrocarbon accumulation in buried hills.

1. Introduction

During the Mesozoic, East Asia was dominated by the collision and subduction of three oceanic plates, including the Paleo-Pacific Ocean, Paleo-Asian Ocean, and Tethys Ocean plates (Li et al., 2012; Ge et al., 2014; Li et al., 2018a; Zheng and Dai, 2018; Suo et al., 2020; Ju et al., 2021), resulting in the compression and thickening of the crust as well as the collapse and thinning of the lithosphere. As a result, there were multiple tectonic transitions in East Asia during this period (Liu et al., 2007; Li et al., 2012; Li et al., 2013; Liu et al., 2013; Meng et al., 2019; Suo et al., 2020). These tectonic transitions were closely related to the Indosinian and Yanshan movements (Liu et al., 2007; Li et al., 2013; Liu et al., 2015; Liu et al., 2017; Yang et al., 2022b). The Indosinian movement was the initial stage of the destruction of the North China Craton (NCC), which was characterized by compressional deformation (Zhao et al., 1994; Zhou et al., 2012; Li et al., 2012; Dong et al., 2016; Wang et al., 2019; Li et al., 2021). However, debate remains concerning the formation and evolution of the main structural styles in this period. Some previous studies suggested that the near E-W and NW-trending folds and reverse faults were formed in response to the near S-N compressive stress during the Indosinian movement period (Zhou et al., 2012; Wang et al., 2019; Li et al., 2019; Li et al., 2021). Others indicated that the formation of the near E-W and NW-trending folds and thrust faults was triggered by a change of stress field from near S-N to NE-SW during the Indosinian movement period (Li et al., 2009a; Li et al., 2009b; Yin and Nie, 1993; Zhang, 1998; Li et al., 2013; Qi et al., 2003; Dong et al., 2011). Follwoing the Yanshan movement during the Late Jurassic to the Early Cretaceous, the destruction of the NCC reached its peak, and the NE- and NNE-trending tectonics were extensively developed, replacing the earlier near E-W and NW-oriented tectonics (Li et al., 2012; Li et al., 2019; Yang et al., 2022b). The Early Yanshan movement was characterized by NE- and NNE-oriented folding and transpressional

* Corresponding author at: College of Geosciences, China University of Petroleum (Beijing), Changping, Beijing 102249, China.
E-mail address: yuxin0707@163.com (Y. Yu).

https://doi.org/10.1016/j.jseaes.2024.106254
Received 8 October 2023; Received in revised form 5 July 2024; Accepted 9 July 2024
Available online 10 July 2024

faulting, while the Late Yanshan movement was mainly dominated by the NE- and NNE-oriented folding (Hsiao et al., 2004; Liu et al., 2017; Feng and Ye, 2018; Li et al., 2019; Li et al., 2021). During the middle period of the Yanshan movement (Late Jurassic-Early Cretaceous), the lithosphere of the NCC was thinned, and large-scale volcanism and magmatic intrusion occurred (Deng et al., 2007; Li et al., 2011; Li and Santosh, 2014; Yang et al., 2018; Li et al., 2019; Ju et al., 2021), resulting in the Mesozoic inverted fault basins.

Until now, much progress has been made in the destruction of the NCC (Gao et al., 2002; Xu, 2007; Zhu et al., 2011; Wu et al., 2019). It is noteworthy, however, that these studies were mainly based on the onshore geological data, and comprehensive research on the Mesozoic evolution of the NCC is still insufficient. The Bohai Bay Basin, with onshore and offshore parts, is located in the eastern NCC. Researchers widely accept that the Bohai Bay Basin was formed during the destruction of the NCC. The basin experienced multiple tectonic movements of compression and extension during the Mesozoic (Cheng et al., 2018; Wang et al., 2019; Suo et al., 2020; Ju et al., 2021; Liu et al., 2022; Wang et al. 2022). The northern Bozhong depression is situated in the juction of NE-, near E-W-, and NW-trending tectonic zones, and has undergone compression, strike-slip, and extension stresses. The three groups of faults with the NE, near E-W, and NW strikes have different structural characteristics, but their evolutionary processes are still controversial. It has been suggested that the near E-W and NW-trending faults were formed as reverse faults during the Late Triassic and changed to normal faults during the Late Jurassic-Early Cretaceous (Liu et al., 2022; Li et al., 2011; Yang et al., 2018; Li et al., 2019; Ju et al., 2021). Zhu et al. (2012) suggested that the inversion of the early near E-W and NW-trending reverse faults was triggered by the back-arc spreading of East Asia during the Late Jurassic-Early Cretaceous. In addition, the left-lateral strike-slipping movement of the NE-trending faults during the Late Jurassic-Early Cretaceous was thought to have induced the inversion of the early near E-W and NW-trending reverse faults (Liu et al., 2022; Li et al., 2011; Yang et al., 2018; Li et al., 2019; Ju et al., 2021). Due to the lack of the high-resolution seismic data in the early period, there were many difficulties in understanding the complex evolutionary history of the northern Bozhong depression. In this study, we focus on the Mesozoic tectonic features of the northern Bozhong depression using the newest 3D seismic data. Based on the systematical analysis of fault activity and balanced cross-section, the evolutionary processes of faults of various strikes and their relationships to the regional tectonic forcings are revealed. Furthermore, the dynamic mechanisms of different structural styles of the northern Bozhong depression are also discussed.

2. Regional geological setting

The Bohai Bay Basin is an important petroliferous basin in the NCC, eastern China (Fig. 1a; Cheng et al., 2018; Wang et al., 2019). The basin is surrounded by the Yanshan fold belt to the south, the Taihang Mountains uplift to the east, the Luxi uplift to the north, and the Jiaoliao massif to the west (Yu et al., 2009, 2020; Li et al., 2019; Ju et al., 2021). The Bohai Bay Basin consists of the Huanghua, Jiyang, Bozhong, Jizhong, and Liaoxi depressions (Fig. 1b; Jiang et al., 2017; Zhu et al., 2021; Fu et al., 2022).

The pre-Cenozoic strata in the Bohai Bay Basin are composed of the Archaean-Proterozoic, Paleozoic, and Mesozoic (Su et al., 2009; Li et al., 2021), documenting the tectonic events of the Indosinian and Yanshan movements in the basin (Li et al., 2012, 2013, 2015; Yang et al., 2016; Zhou et al., 2017; Zhu et al., 2019a; Lu et al., 2022). The Mesozoic movements in the Bohai Bay Basin can be divided into five major stages, including the Early Indosinian movement at the end of the Middle Triassic, the Late Indosinian movement in the Late Triassic, the Early Yanshan movement in the Early-Middle Jurassic, the Middle Yanshan movement in the Late Jurassic-Early Cretaceous, and the Late Yanshan movement in the Late Cretaceous (Li et al., 2013; Cheng et al., 2018; Li et al., 2021). During the Early Indosinian period, regional uplift occurred in the Bohai Bay Basin, resulting in the near EW-trending broad and gentle folds (Li et al., 2015; Dong et al., 2016; Cheng et al., 2018; Dmitrienko et al., 2018; Li et al., 2019). During the Late Indosinian period, the eastern Bohai Bay Basin experienced NW- and NNW-oriented folding and thrusting, which was superimposed on the near EW-trending folds of the Early Indosinian period. In contrast, inheriting the structural

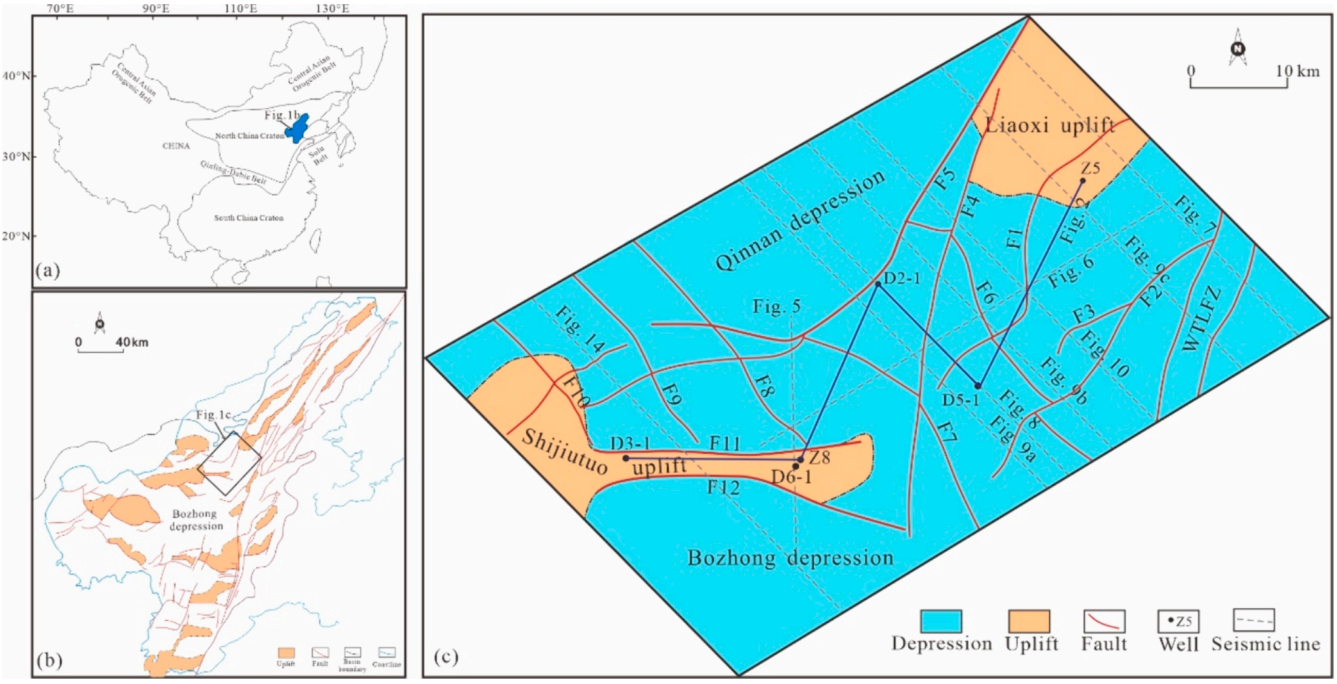

Fig. 1. (a) Simplified map of tectonic framework of the North China Craton and location of the Bohai Bay Basin (Modified after Wu et al., 2019). (b) Map showing the tectonic setting of the Bohai Bay Basin and the location in the study area (Modified from Ye et al., 2019). (c) Map showing the structural features of the northern Bozhong depression.

deformation of the Early Indosinian folding, the western basin had a weaker deformation intensity (Cheng et al., 2018; Liu et al., 2022). In the Early Yanshan period, the whole basin was still dominated by the compressional background, forming NNE-oriented folds and thrust faults. In addition, the NNE-trending faults, such as the Tanlu fault zone (TLFZ), initiated as a result of the sinistral strike-slip motion (Li et al., 2012; Zhang et al., 2015; Ju et al., 2021). Triggered by the thinning and collapse of the lithosphere during the Middle Yanshan period, the Bohai Bay Basin and its surrounding areas entered the extensional stage of rifting and inversion, accompanied by strong volcanic activities. The early near EW-, NW- and NNE-trending thrust faults were inverted to form the Mesozoic fault basins along different strikes (Li et al., 2011; Yang et al., 2019). Again, the Bohai Bay Basin entered into a compressional setting during the Late Yanshan period, and uplift occurred in some local areas. The Mesozoic NE- and NNE-trending fault basins began to invert, and the basin was characterized by NE- and NNE-trending fold deformation (Cheng et al., 2018; Li et al., 2021; Lu et al., 2022).

The study area is located of the northern Bozhong depression, where several uplift zones of metamorphic buried hills are well preserved (Fig. 1c). The complex Mesozoic fault system of the northern Bozhong depression is composed of reverse, normal, transtensional, and inversion faults of the NE, near E-W, and NW strikes (Zhang et al., 2019; Wang et al., 2021; Yang et al., 2022a). The Mesozoic evolution of the faults can be divided into several stages, including the compressional stage during the Indosinian and the Early Yanshan periods, the extensional stage during the Middle Yanshan period, and the compressional stage in the Late Yanshan period (Zhang et al., 2019; Wang et al., 2021; Yang et al., 2022a).

The Archean metamorphic granite was widely developed in the study area (Fig. 2; Zhang et al., 2019; Yang et al., 2022a). The Proterozoic strata in the southern study area are typically composed of marine metamorphic quartz sandstone with glauconite, which is thin and similar to that in the Miaoxi, Shaleitian, and Bonan Low uplifts (Fig. 2; Wang et al., 2021; Yang et al., 2022a). The Cambrian-Ordovician strata are dominated by marine carbonates. However, the Silurian-Devonian strata are poorly preserved. The Carboniferous and the Permian comprise terrigenous clastic rock with thin coal seams at the base (Fig. 2; Zhang et al., 2019; Wang et al., 2021; Yang et al., 2022a). Although the thickness of the Mesozoic is enormous, the Triassic, the Lower-Middle Jurassic, and the Upper Cretaceous strata are absent (Zhang et al., 2019; Wang et al., 2021; Yang et al., 2022a). The Upper Jurassic-Lower Cretaceous are dominated by volcanic breccia, while the Middle Cretaceous strata are characterized by clastic rock and tuff (Fig. 2; Zhang et al., 2019; Wang et al., 2021; Yang et al., 2022a). The Cenozoic strata are well developed in the study area (Fig. 2; Zhang et al., 2019; Wang et al., 2021; Yang et al., 2022a).

3. Data and method

The new 3D seismic and drilling data, which covers an area of 3,000 km^2, are used in this study. The 3D seismic survey covers the eastern Shijiutuo uplift, the southern Liaoxi uplift, the eastern Qinnan depression, and the northern Bozhong depression, parts of which are shown in this study (Fig.). In addition, the correlation between seismic profiles and drilling data was employed to generate synthetic seismic records and to calibrate the stratigraphic boundaries, which proved to be a valuable tool for enhancing the accuracy of 3D seismic interpretation. The spatial distribution of different strata was analyzed through the well profiles and contour maps of the residual strata. The interpretation of seismic data and geological mapping were conducted by the Landmark software. During the seismic interpretation, some previous structural models from articles and unpublished internal reports were reviewed. The balanced section method and 3Dmove software were employed to rebuild the Mesozoic tectonic evolution of the northern Bozhong depression.

4. Results

4.1. Mesozoic stratigraphic characteristics of the northern Bozhong depression

4.1.1. Seismic stratigraphy

The pre-Cenozoic strata of the northern Bozhong depression can be divided into three mega-sequences, including the Archaean-Proterozoic, the Paleozoic, and the Late Jurassic-Early Cretaceous sequences. Based on the comprehensive analysis of drilling and seismic reflection data, the seismic reflection characteristics of different strata and lithologies have been clearly identified (Fig. 3). The Archaean-Proterozoic strata are featured by the chaotic and discontinuous reflection, with low-frequency and weak-amplitude in seismic profiles (Fig. 3). The lower part of the Paleozoic strata are characterized by parallel, continuous, mid-frequency, and medium-strength amplitude reflections, while the upper part are featured by more continuous, mid-frequency, and medium-strength amplitude reflections (Fig. 3). The Upper Jurassic-Lower Cretaceous strata comprise volcanic rocks and volcanic clastic rocks. In seismic profiles, the volcanic rocks are mixed, disorderly, and discontinuous, with medium frequency and medium-strength amplitude. The volcanic clastic rocks, however, are parallel and continuous, with medium frequency and medium-strength amplitude reflections (Fig. 3).

The unconformity usually records the history of regional tectonic movements and directly reflects the tectonic transition processes. Based on the termination relationships of seismic reflection, three key angular unconformities have been identified from the northern Bozhong depression. The unconformities were formed between the Precambrian and the overlying strata, the Paleozoic and Upper Jurassic-Lower Cretaceous strata, and the pre-Cenozoic and the Cenozoic strata (Fig. 3).

4.1.2. Spatial distribution of strata

According to the characteristics of the seismic facies of different strata and the termination relationships of the seismic reflections, the sequence stratigraphic framework of the northern Bozhong depression is established. The results of seismic interpretation show that the Paleozoic strata is widely absent in the central area. The Liaoxi uplift in the northern area is relatively stable during the Paleozoic, and the distribution of the Paleozoic in the eastern Shijiutuo uplift is relatively complicated, where the Paleozoic is pinched from the west to the east and becomes thinner in the higher part of the uplift (Fig. 4a). The Upper Jurassic-Lower Cretaceous strata are widely distributed in the northern Bozhong depression, and they are just absent in the eastern Shijiutuo uplift and local area of the Liaoxi uplift. The strata are distributed along the near E-W orientation in the southern area and the NE and NNE orientation in the northern and central areas (Fig. 4b). The variation features between the thicknesses of the Paleozoic and Mesozoic strata are obviously different. The Mesozoic thickens close to the hanging walls of faults, but the Paleozoic becomes thinner close to the hanging walls (Fig. 4).

4.2. Mesozoic structural deformation

4.2.1. Compressional structures

Different types of the early compressional structures, such as back-thrust faults, imbricate thrust structures, positive flower structures, and anticlines had been identified in the study area.

The SN-orientation seismic sections show that there are a group of near EW-trending listric normal faults, which cut from the Precambrian to the Cenozoic strata, such as the eastern boundary faults of the Shijiutuo uplift (F11 and F12 in Fig. 5). The Paleozoic covers over the Archaean-Proterozoic in the Shijiutuo uplift, where the Triassic strata are poorly preserved. The Paleozoic becomes thinner toward the near E-W faults, while the Upper Jurassic-Lower Cretaceous strata thicken toward the E-W faults. It can be inferred that the near E-W faults were

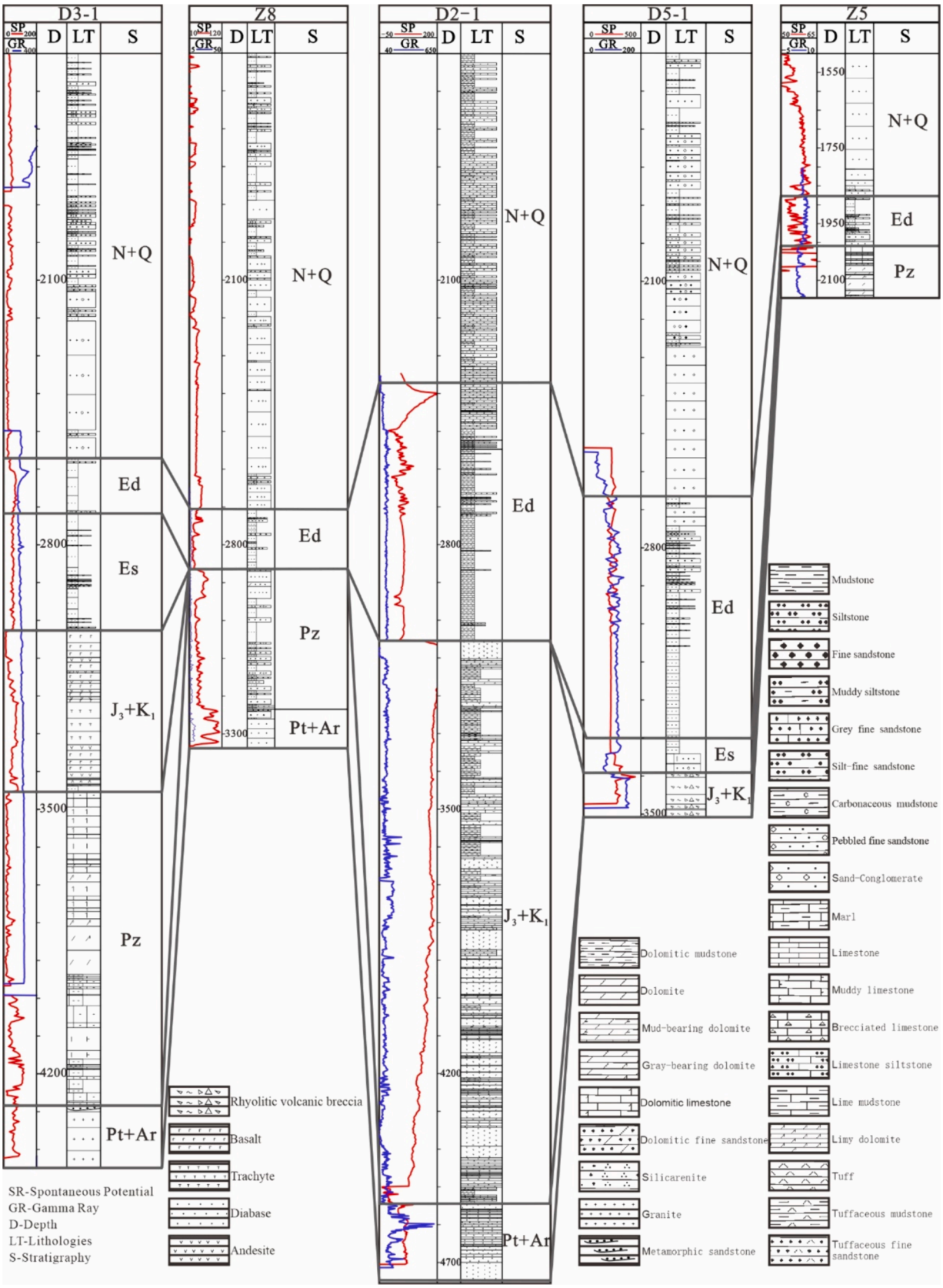

Fig. 2. Correlation section through the wells D3-1, Z8, D2-1, D5-1, and Z5 of the northern Bozhong depression. Well locations are shown in Fig. 1c.

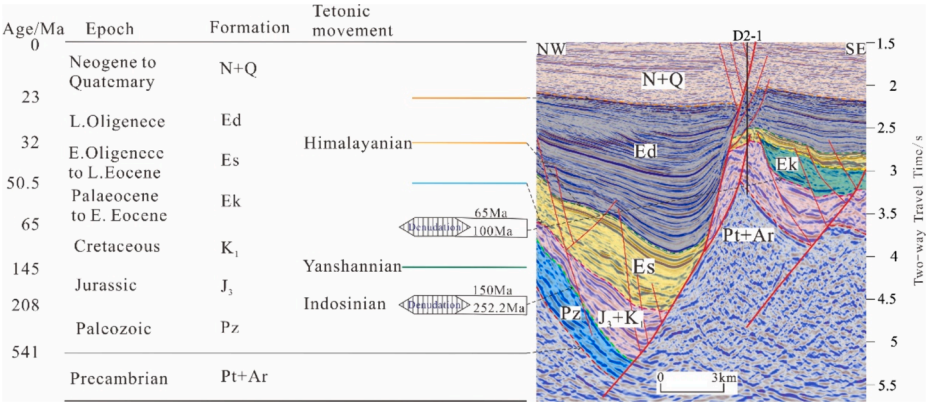

Fig. 3. Seismic stratigraphic framework of the northern Bozhong depression with the interpreted seismic sections of Fig. 8. See Fig. 1c for its location. Abbreviation: Pt + Ar, Archean-Proterozoic; ∈+O, Cambrian-Ordovician; C + P, Carboniferous-Permian; J_3, Upper Jurassic; K_1, Lower Cretaceous; Ek, Kongdian Formation; Es, Shahejie Formation; Ed, Dongying Formation; N + Q, Neogene-Quaternary.

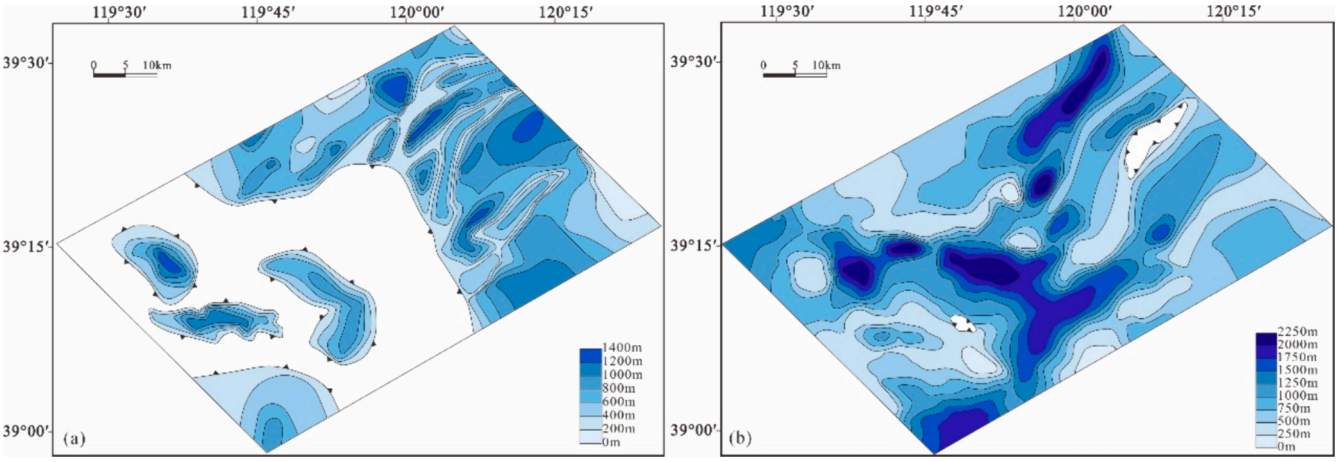

Fig. 4. Isopach maps of the Mesozoic (a) and the Paleozoic (b) of the northern Bozhong depression.

back-thrust faults before the Late Jurassic, resulting in local denudation of the Paleozoic in the hanging walls. During the Late Jurassic-Early Cretaceous, the inversion of the near E-W faults formed a near E-W Mesozoic faulted sag (Fig. 5). The EW-trending back-thrust faults controlled by S-N compression stress are only developed in the southern area.

As shown in the NE-SW seismic sections, the imbricate thrust faults cut from the Precambrian to the Mesozoic strata (Fig. 6). The Paleozoic strata have a wedge shape and are thinning toward the hanging walls of the NW-trending faults. However, the Triassic strata are absent in the northern Bozhong depression. The Upper Jurassic-Lower Cretaceous strata overlap on the Paleozoic, and thicken toward the E-W faults. Controlled by the strong compression stress, the imbricate thrust structures were formed during the Late Triassic. In addition, the strong denudation of the Paleozoic sequences occurred within the NW-trending faults, and the near NW-trending faults of the Late Jurassic-Early Cretaceous were inverted to form the Mesozoic faulted sags (Fig. 6). The NW-trending thrust structures were only developed in the central area, which was probably to be influenced by the NE-SW compression stress.

The Paleozoic anticlines with NE- and NNE-trending axes have developed in the northern area, whose cores and limbs have thin and thick Paleozoic thickness, respectively. There is a significant unconformity between the Jurassic-Lower Cretaceous and the Paleozoic successions (Fig. 7). According to the stratigraphic thicknesses and fault features, it can be inferred that the Early-Middle Jurassic flower structure, with an NE strike, was probably affected by transpressional stress, and the Paleozoic in the core of the anticline was seemed to be suffered from strong denudation. During the Late Jurassic-Early Cretaceous, the NE-trending flower structure was inverted, and the strata were deposited simultaneously (Fig. 7). A significant angular unconformity developed between the Upper Jurassic-Lower Cretaceous and the Paleogene sequences (Fig. 8). Under the unconformity, the Upper Cretaceous strata are absent, and the Upper Jurassic-Lower Cretaceous strata are obviously truncated. The overlying Paleogene strata overlap on this unconformity (Fig. 8). It is inferred that the anticline was probably formed during the Late Cretaceous. Influenced by the NW-SE compression stress, the Mesozoic strata were folded and uplifted, leading to the absence of the Upper Cretaceous (Fig. 8).

4.2.2. *Strike-slip structures*

As shown in Fig. 9, the NE- and NNE-trending strike-slip faults, such as the F4, F5, and the western branch of the TLFZ (WTLFZ), were mainly developed in the northern and central areas. The strike-slip faults are clearly segmented, and the dip angles of the faults gradually steepen from south to north. The faults have an upright shape and flower-like structural features in the northern and southern sectors, respectively (Fig. 9). It can be concluded that the northern faults were mainly affected by shear, and the southern sectors were jointly controlled by shear and extension. The faults F4 and F5 cut through the Precambrian to the Cenozoic strata, and the Upper Jurassic-Lower Cretaceous strata in the hanging walls thicken towards the faults, which shows a Mesozoic

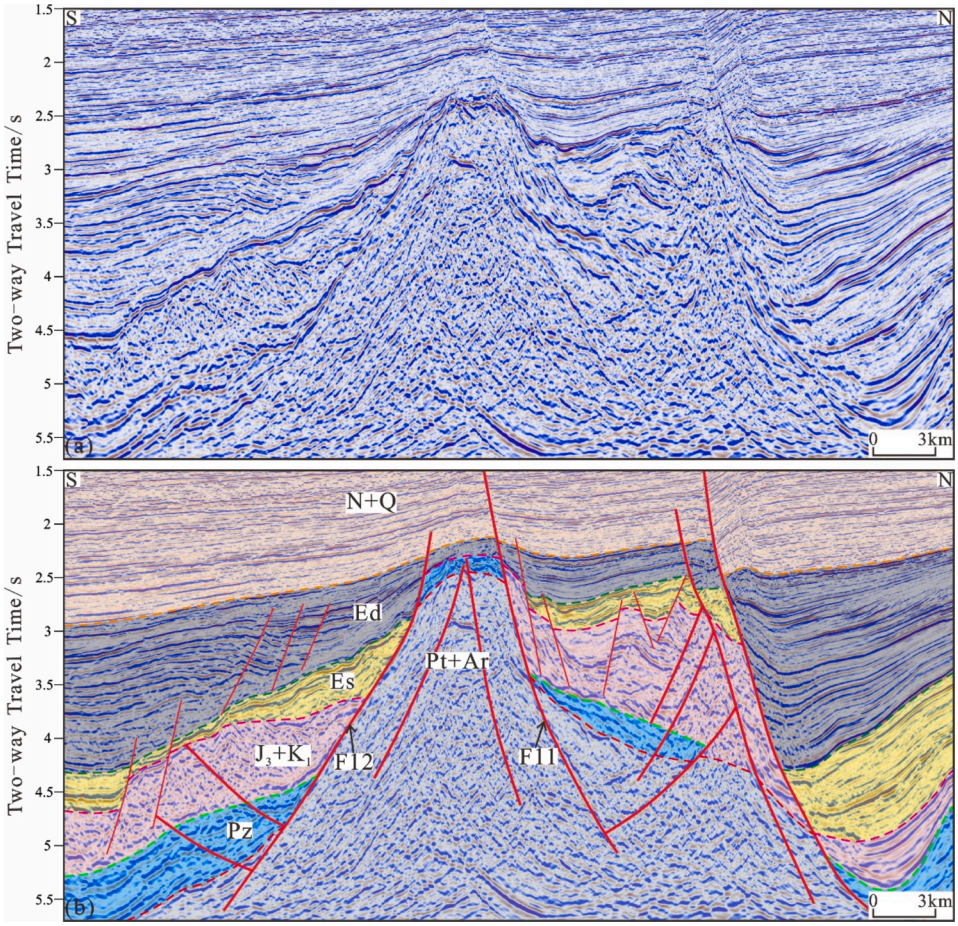

Fig. 5. (a) Uninterpreted and (b) interpreted south-northward seismic profiles. Line location is shown in Fig. 1c.

initiation of these faults (Fig. 9).

4.2.3. *Extensional structures*

As seismic profiles shown in Fig. 10, the NE- and NNE-trending extensional faults had controlled the formation of buried hills. Faults with combination styles of domino and "Y" shapes, cut from the pre-Cambrian to the Cenozoic strata (Fig. 10). The thickness of the Mesozoic in the hanging walls of the NE- and NNE-trending extensional faults is thicker than that in the footwalls, indicating a initiation of these faults during the Mesozoic (Fig. 10).

4.3. *Characteristics of fault development*

The three groups of faults in the northern Bozhong depression experienced multiple phases activities (Fig. 11). During the Middle-Late Triassic, the near EW- and NW-trending faults started to be active, with thrust rates ranged from 8.9 to 18.8 m/Ma, and then declined during the Early-Middle Jurassic (Fig. 11). The activity rates of the NW- and near EW-trending faults in the Late Jurassic-Early Cretaceous increased significantly (Fig. 11). It can be concluded that the early thrust faults were inverted to be normal faults during this time. Influenced by the NW-SE extension stress, the NE-trending normal faults were also developed in this period. During the Late Cretaceous, the NW-, near E-W, and NE-trending faults were continuously active, but they were characterized by reverse faults (Fig. 11).

The strikes and types of the *syn*-depositional faults of the northern Bozhong depression varied obviously through time (Fig. 12). During the Middle-Late Triassic, the EW- and NW-trending *syn*-depositional reverse faults were developed in the southern and central areas (Fig. 12a and 12b). Thrust faults with opposite dips were also formed on the northern and southern sides of the Shijiutuo uplift, resulting in a combination of near EW-trending back thrust faults (Fig. 12a). In the southern and central areas, imbricate thrust structures were formed by a series of NW-striking reverse faults with the same dips (Fig. 12b). During the the Lower-Middle Jurassic, sinistral strike-slip faults with a NE strike developed in the northern and central areas. The early near EW- and NW-trending reverse faults continued to active, but their intensity was obviously weak (Fig. 12c). During the Late Jurassic-Early Cretaceous, the EW- and NW-trending reverse faults were inverted to be normal faults. In addition, the NE-trending normal faults were developed in the northern and central areas, and the early sinistral strike-slip faults were still active during this time (Fig. 12d). During the Mesozoic, the predominant strikes of the faults gradually changed from the EW to NW and then NE from south to north in study area.

4.4. *Mesozoic tectonic evolution of the northern Bozhong depression*

Following the compression, shear and extension stresses in different periods, the northern Bozhong depression had undergone complex multi-phase structural deformation, resulting in the regional strata denudation and areas changes in cross-sections. In this study, the conservation of the stratigraphic areas in profiles was achieved by restoring the amount of regional strata denudation based on a balanced cross-section restoration (Gibbs, 1983; Cheng et al., 2018; Liu et al., 2022). Here, two typical seismic profiles are employed to analyze the characteristics of the Mesozoic tectonic movements in northern Bozhong depression (Figs. 13 and 14).

Response to the Indosinian and Yanshan movements and associated Mesozoic compressional tectonic activities, two obvious angular unconformities developed in northern Bozhong depression between the

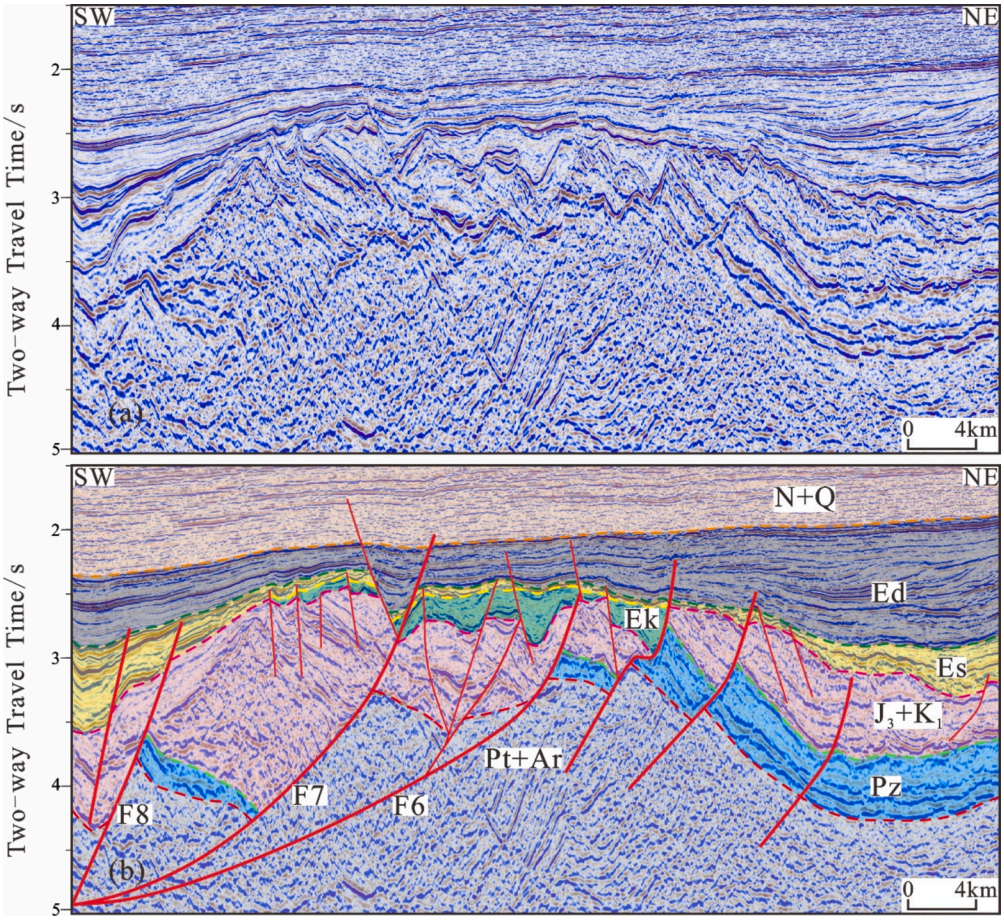

Fig. 6. (a) Uninterpreted and (b) interpreted northeast-southwestward seismic profiles. Line location is shown in Fig. 1c.

Paleozoic and the Upper Jurassic-Lower Cretaceous, and the Upper Jurassic-Lower Cretaceous and the Paleogene, respectively (Zhang et al., 2019; Wang et al., 2021; Yang et al., 2022a).

The balanced restoration of the cross-section, across the northern and central areas, reveals that the tectonic background of study area was relatively stable, and there was no folding and faulting after the deposition of the Lower-Middle Triassic (Fig. 13f). In the Late Triassic, the NW-trending faults and fault-related anticlines were formed in response to the Indosinian movement, and resulted in the absence of the Triassic and the local denudation of the Paleozoic strata (Fig. 13e). During the Early Yanshan period (the Early-Middle Jurassic), the study area was still under the influence of compression stress. The NW-trending thrust faults continued to be active, and several NE-trending strike-slip faults were widely formed. Consequently, the Lower-Middle Jurassic strata were absent in the northern and central areas (Fig. 13d). During the Middle Yanshan period (the Late Jurassic-Early Cretaceous), the early NW- and NE-trending thrust faults were inverted under the extensional tectonic background. Meanwhile, some new NE-trending normal faults were formed. Mesozoic faulted sags with different trends were formed as a result of fault activities during this time (Fig. 13c). Subsequently, the pre-Paleogene strata were folded and uplifted under the compressional environment during the Late Yanshan period in the Late Cretaceous, resulting in the absence of the Upper Cretaceous strata. The angular unconformity between the pre-Paleogene and Paleogene strata can also demonstrate the Late Yanshan movement (Fig. 13b).

In the southern area, the Lower-Middle Triassic strata were deposited stably (Fig. 14f). In the late Middle Triassic, the near EW-trending reverse faults and folds were formed, leading to the absence of the Lower-Middle Triassic in the southern area and local denudation of the Paleozoic strata (Fig. 14e). The near E-W reverse faults continued to be active in the Late Triassic. The Upper Triassic strata were not deposited in the southern area, and the Paleozoic strata were furtherly denuded. During the Early-Middle Jurassic, the near E-W reverse faults were still active and the southern area was suffered from compression and uplift, and the Lower-Middle Jurassic strata were not deposited at this time (Fig. 14d). In the Late Jurassic-Early Cretaceous, the stretching activity of near E-W faults occurred, and the thick Upper Jurassic-Lower Cretaceous strata were deposited, suggesting an extensional tectonic environment in the southern area (Fig. 14c). In the Late Cretaceous, the Mesozoic strata in the southern area were folded, and the Upper Cretaceous strata were absent. In addition, the Upper Jurassic-Lower Cretaceous strata were partly denuded, indicating a compressional background in the southern area at this time (Fig. 14d).

The results of balanced section restoration are shown in Table 1 and Figs. 13 and 14. The shortening rates of profiles of various directions from the Late Triassic to the Early-Middle Jurassic are negative. The shortening rates of the southern and the northern-central sections are 4.72 % and 3.32 %, respectively (Table 1). In contrast, the Late Jurassic-Early Cretaceous extension rates of these two sectionsare 39.18 % and 10.65 %, respectively (Table 1). During the Late Cretaceous, the extension rates of the two sections varied to be negative, indicating a compressional background in study area. The deformation in the southern area was much stronger than that in the northern and central areas at this time.

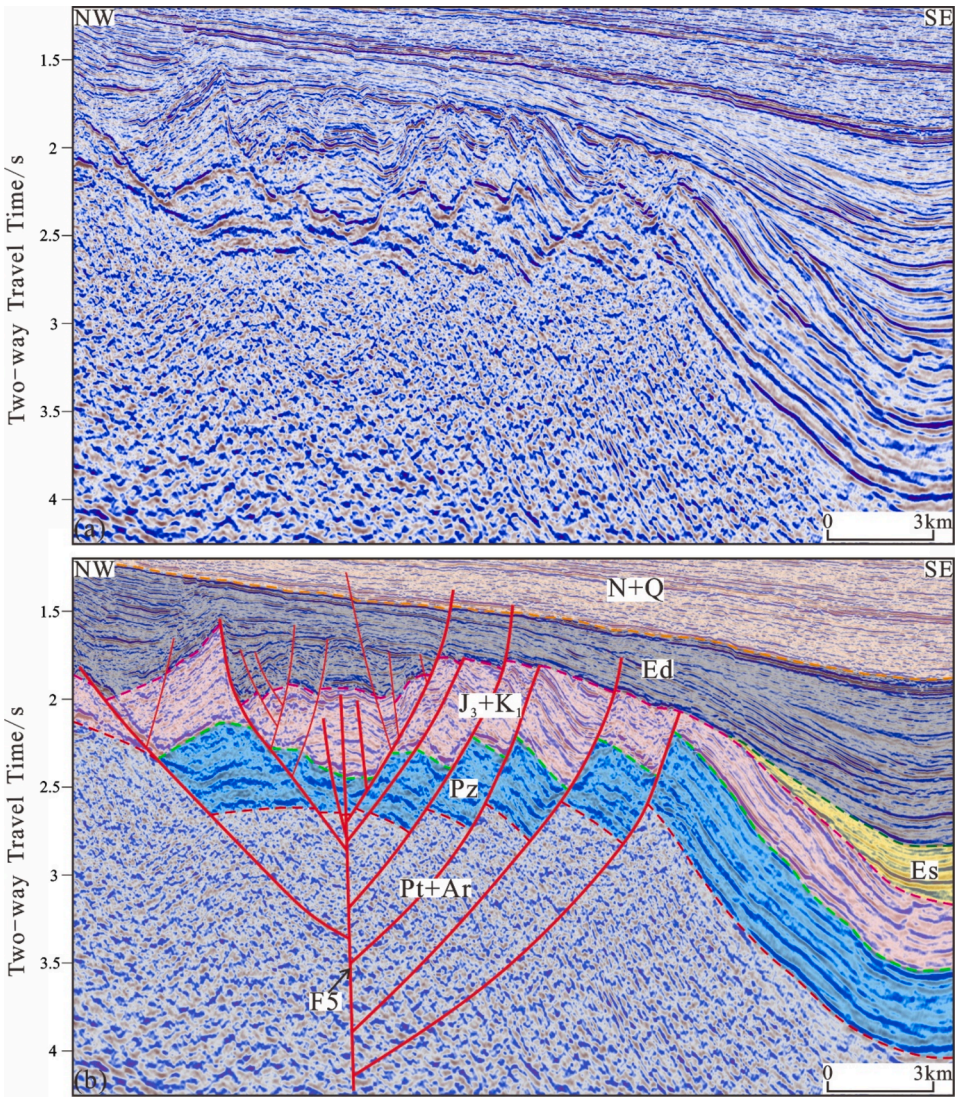

Fig. 7. (a) Uninterpreted and (b) interpreted northwest-southeastward seismic profiles showing negative flower structure. Line location is shown in Fig. 1c.

5. Discussion

5.1. Mesozoic tectonic evolution processes and formation mechanisms

5.1.1. Compressional stage during the Middle-Late Triassic

Debate continues concerning the structural features of the Triassic in eastern China. Some studies proposed that a series of near E-W and NW-trending folds and thrust faults were developed in the near S-N compression stress field in the Late Triassic (Li et al., 2000; Zhou et al., 2012; Wang et al., 2019; Li et al., 2019; Li et al., 2021). Other researchers have divided the tectonic evolution processes of the Triassic eastern China into two different stages. The first stage is the near S-N compressional stage at the end of the Middle Triassic. During this stage, the South China plate was subducted under the North China plate along the SSW direction, and large near E-W broad and gently anticlines and thrust faults were formed (Fig. 15a; Li et al., 2009a; Li et al., 2009b; Yin and Nie, 1993; Qi et al., 2013). For the second stage of the Late Triassic, the direction of the compression stress field changed to the NE-orientation. During this stage, clockwise rotation occurred in the South China plate, and the Paleo-Tethys Ocean closed with the scissors-type from east to west. The local compressional direction within the plate was adjusted to the NE-SW, forming the NWW-trending Qinling-Dabie orogenic belt (Fig. 15b; Li et al., 2009a; Li et al., 2009b; Yin and Nie, 1993; Zhang, 1998; Li et al., 2013; Qi et al., 2003; Dong et al., 2011). The zircon U-Pb dating results of the high-pressure basic granulite in the Mianlue area and the overpressure eclogite in the eastern Qinling Tectonic Belt are about 200 Ma and 230 Ma, respectively, indicating the late Middle-Late Triassic collision between the South China and the North China plates (Li et al., 2000; Hacker et al., 1998; Dong et al., 2011). As the collisional stress transmitted to the Bohai Bay Basin, several near E-W broad and gentle anticlines, NW-trending folds and thrust faults were formed in the basin, such as the Xiaozhan-Beidagang-Shaleitian structural belt and the Gusi-Chengnan fault zone (Qi et al., 2003; Wu et al., 2007). The balanced cross section shows that the near E-W and NW folds and faults were developed well during the Triassic of the northern Bozhong depression, suggesting a structural deformation controlled by the near S-N and NE compression stresses during this period. The Triassic strata were absent in the study area, but the Paleozoic strata were preserved in some local areas. The distribution of the Paleozoic strata shows that the near E-W and NW compression occurred in the study area. In addition, the unconformity between the Paleozoic and the Mesozoic strata suggests that the thrust tectonic movement occurred in the northern Bozhong depression during the Triassic.

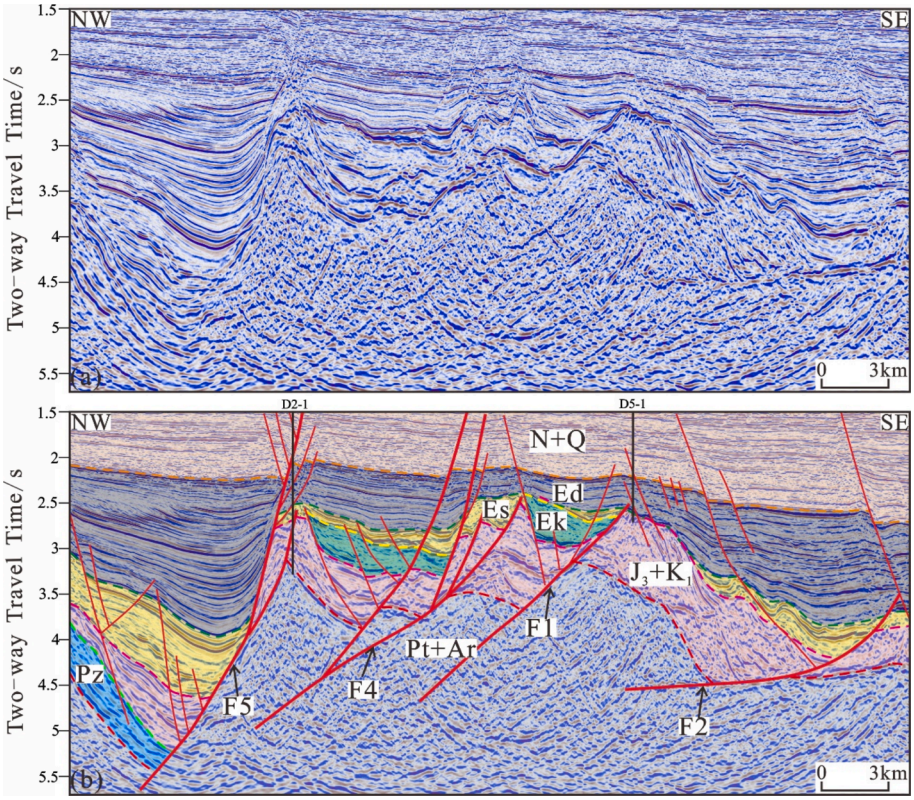

Fig. 8. (a) Uninterpreted and (b) interpreted northwest-southeastward seismic profiles. Line location is shown in Fig. 1c.

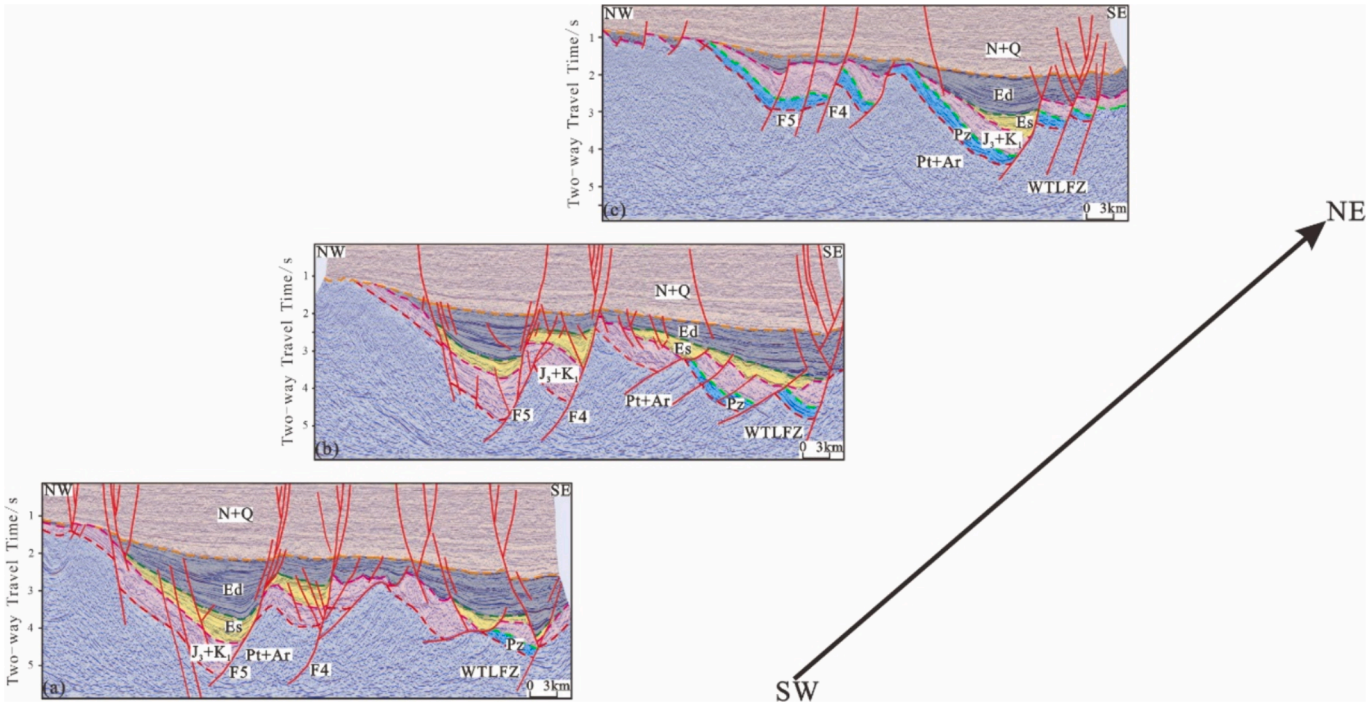

Fig. 9. Interpreted northwest-southeastward seismic profiles across the northern Bozhong depression show the major strike-slip faults. Lines locations are shown in Fig. 1c.

5.1.2. Compressional stage during the Early-Middle Jurassic

It has been demonstrated that the collision between the South China and North China plates gradually weakened during the Early-Middle Jurassic (Liu et al., 2013, 2017; Liu et al., 2022), while the subduction of the Izanagi plate towards the North China plate gradually strengthened. Consequently, the eastern China is interpreted to entered the transition from the Tethys tectonic domain to the Pacific Ocean tectonic domain, and the NCC was dominated by stresses with different directions (Liu et al., 2013, 2017; Dmitrienko et al., 2018; Ju et al., 2021; Li et al., 2021; Liu et al., 2022). During the Early-Middle Jurassic,

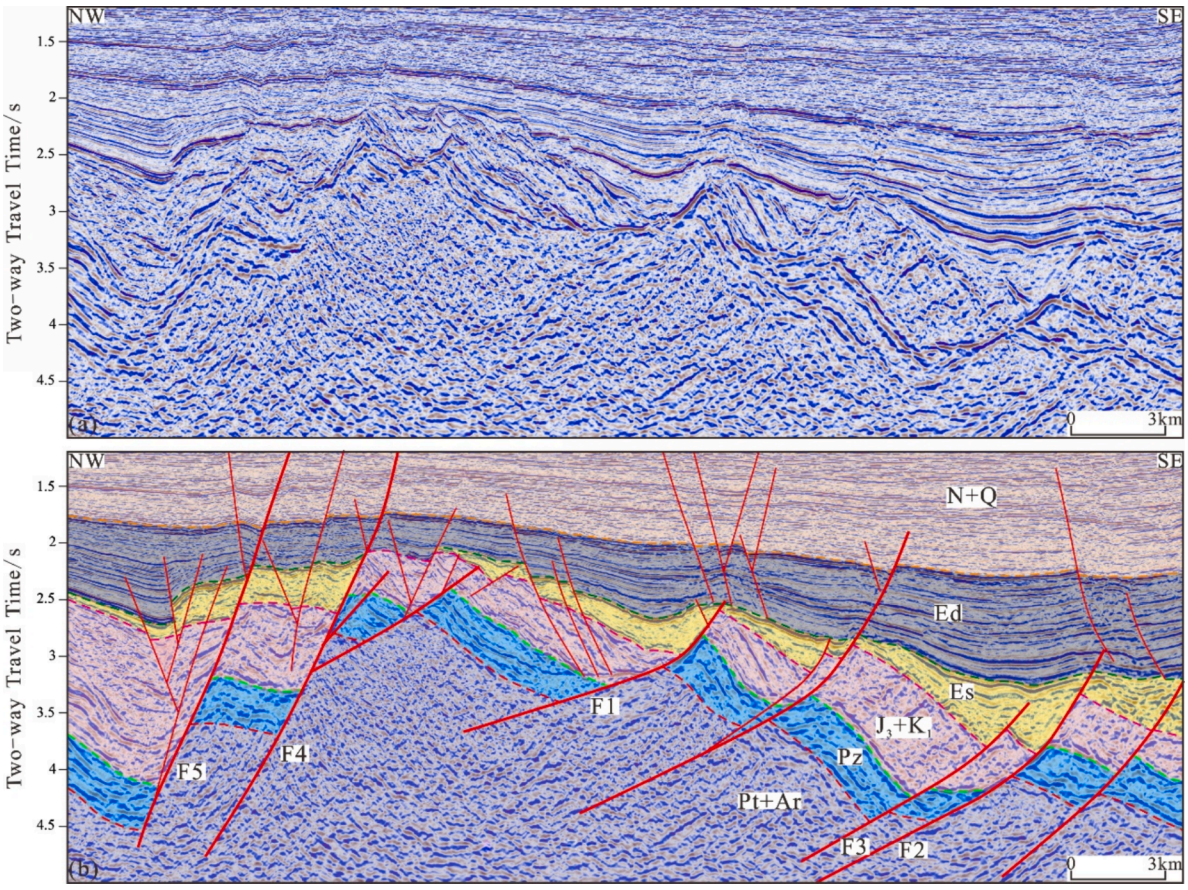

Fig. 10. (a) Uninterpreted and (b) interpreted northeast-southwestward seismic profiles showing compressional structure. Line location is shown in Fig. 1c.

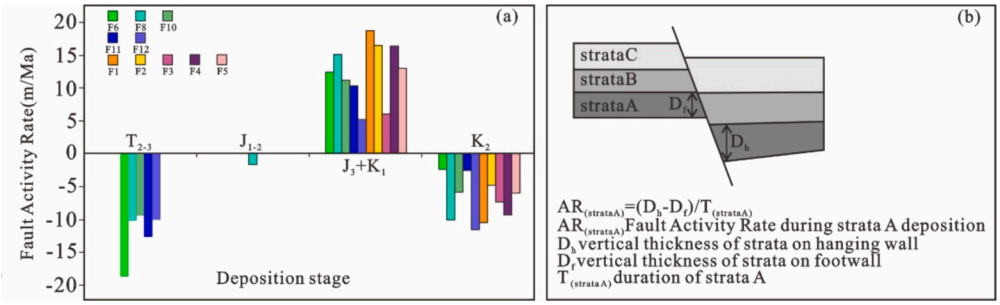

Fig. 11. (a) Activity rates of the three groups of faults during different periods of the northern Bozhong depression. The locations of the faults are shown in Fig. 1c. (b) Map showing the calculation methodology of the fault activity rate (Huang et al., 2014).

following the Izanagi plate subduction towards the North China plate with a high speed and a low angle, and the left-lateral strike-slipping movements occurred in the TLFZ (Fig. 15c; Zhang et al., 2018; Zhu et al., 2018), resulting in the formation of a series of NE- and NNE-trending structural styles in the Bohai Bay Basin (Zhu et al., 2019b). At this time, the NCC was still in the compressional environment, and the Lower-Middle Jurassic strata were limitedly deposited in the Jiyang, Jizhong, and Huanghua depressions, whereas the strata were absent in the study area, northern Bozhong depression (Qi et al., 2003; Wu et al., 2007). The compressional background of the Early-Middle Jurassic Bohai Bay Basin was also proved by the Middle Jurassic adakite in several wells (Ju et al., 2021; Li et al., 2012). The balanced cross-section shows that the northern Bozhong depression was subjected to the NW-SE compression stress in the Early-Middle Jurassic. In the southern and central study areas, the early EW- and NW-trending Paleozoic anticlines and thrust faults with inherited activity were uplifted continuously, and NE- and NNE-trending transpressional faults were developed in the northern study area. The absence of the Lower-Middle Jurassic in the study area also indicates that the structural deformation and deposition was controlled by the compression stress during the Early-Middle Jurassic.

5.1.3. Transtension-negative inversion stage during the Late Jurassic-Early Cretaceous and uplift and denudation stage during the Late Cretaceous

The magmatism and sedimentation during the Late Jurassic-Early Cretaceous indicate that there was an extensional tectonic setting in the NCC (Zhu et al., 2015a; Zhu et al., 2019a; Wang et al., 2018). During the Late Jurassic-Early Cretaceous, the subduction of the Izanagi plate beneath the Eurasian plate from the NNW induced the back-arc spreading (Zhu et al., 2012), and furtherly resulted in the lithosphere thinning and mantle plume activity in the NCC (Ju et al., 2021; Xu, 2007). Some researchers indicated that the rapid rollback of the Paleo-

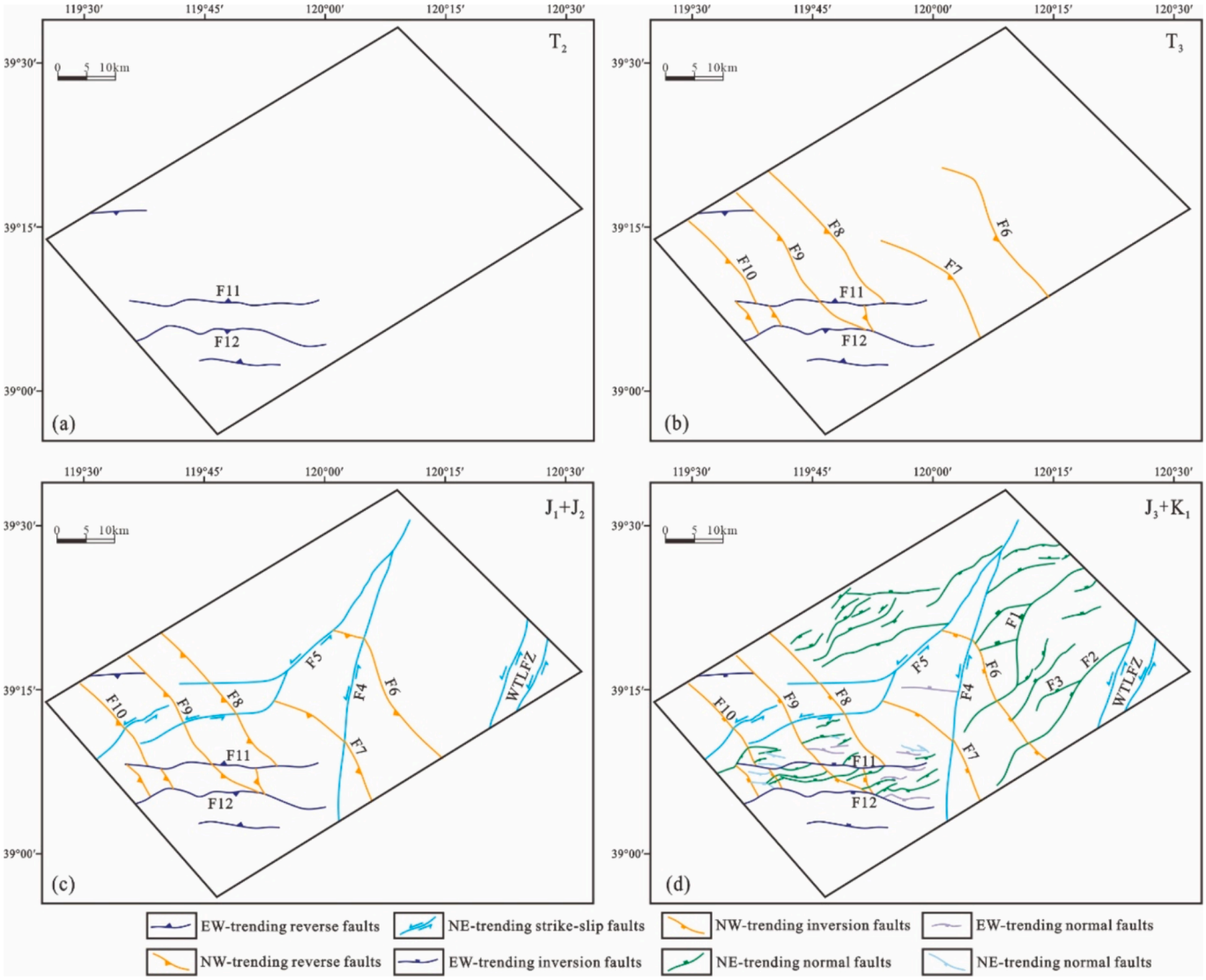

Fig. 12. Distribution of *syn*-depositional faults in different periods. (a)The Middle Triassic, (b)The Late Triassic, (c) The Early-Middle Jurassic, and (d) The Late-Jurassic to Early-Cretaceous.

Pacific plate during 135 to 115 Ma (Fig. 15d; Xu et al., 2012) induced the strong lithospheric extension of the NCC, accompanied by large-scale magmatism (Zhu et al., 2015b; Li et al., 2018b; Wu et al., 2019). During the oblique subduction of the Izanagi plate, a left-lateral strike-slipping event occurred in the NNE-trending TLFZ, resulting in the inversion of the early near E-W and NW thrust faults and the formation of the near E-W, NW, and NE fault basins (Liu et al., 2022; Li et al., 2021; Yang et al., 2018; Li et al., 2019; Ju et al., 2021). The seismic profiles and thickness maps of the Upper Jurassic-Lower Cretaceous strata show a significant control of the near E-W and NW faults on the thick Upper Jurassic-Lower Cretaceous strata in the study area (Fig. 4). The balanced cross section reveals that the near E-W and NW-trending faults in the study area were reverse faults during the Triassic-Middle Jurassic, and then changed to the normal faults during the Late Jurassic-Early Cretaceous. The phenomenon is relatively common in the Bohai Bay Basin (Liu et al., 2022; Ju et al., 2021; Suo et al., 2020). The absence of the Upper Cretaceous strata, as well as the formation of several NE- and NNE-trending anticlines from the central NCC to the western TLFZ (Li et al., 2021), indicates a changed of the tectonic setting from extension to compression in the Late Cretaceous eastern NCC (Wang et al., 2018; Li et al., 2012). In the Late Cretaceous, the magmatism in the NCC was basically quiescent (Liu et al., 2022), and the Izanagi plate subducted horizontally towards the eastern China, resulting in the uplift and denudation of the Mesozoic basins in the NCC, and the left-lateral strike-slipping event of the TLFZ (Fig. 15e; Liu et al., 2022). The drilling data and seismic profiles demonstrate the absence of the Upper Cretaceous strata and the unconformity between the Upper Jurassic-Lower Cretaceous strata and the Paleogene of the northern Bozhong depression, indicating the compressional tectonic background during the Late Cretaceous.

5.2. *Influence of tectonic activities of multiple phases on hydrocarbon accumulation*

The study area is adjacent to the Bozhong and Qinnan depressions, which are important hydrocarbon-rich kitchens in the Bohai Bay Basin. Up to now, oil and gas have been found in the Mesozoic, Paleozoic, and Archean strata in the study area (Fig. 16). Hydrocarbon accumulation in deep strata of the northern Bozhong depression is closely related to Mesozoic fault activities. The discovery wells are mostly located near the main E-W, NE-, and NW-trending faults. The faults have experienced multiple transitions of compression and extension stresses, resulting in the formation of faulted-anticlinal and faulted-horst traps along the faults.

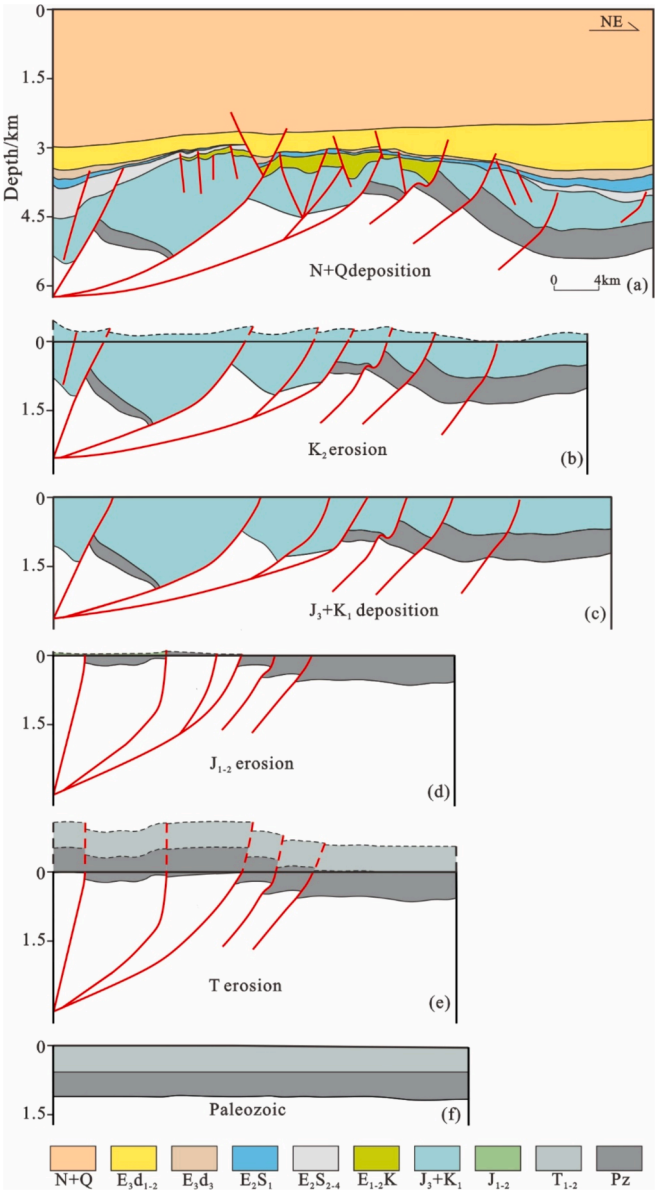

Fig. 13. Balanced restoration of the northeast-southwestward profile in Fig. 6.

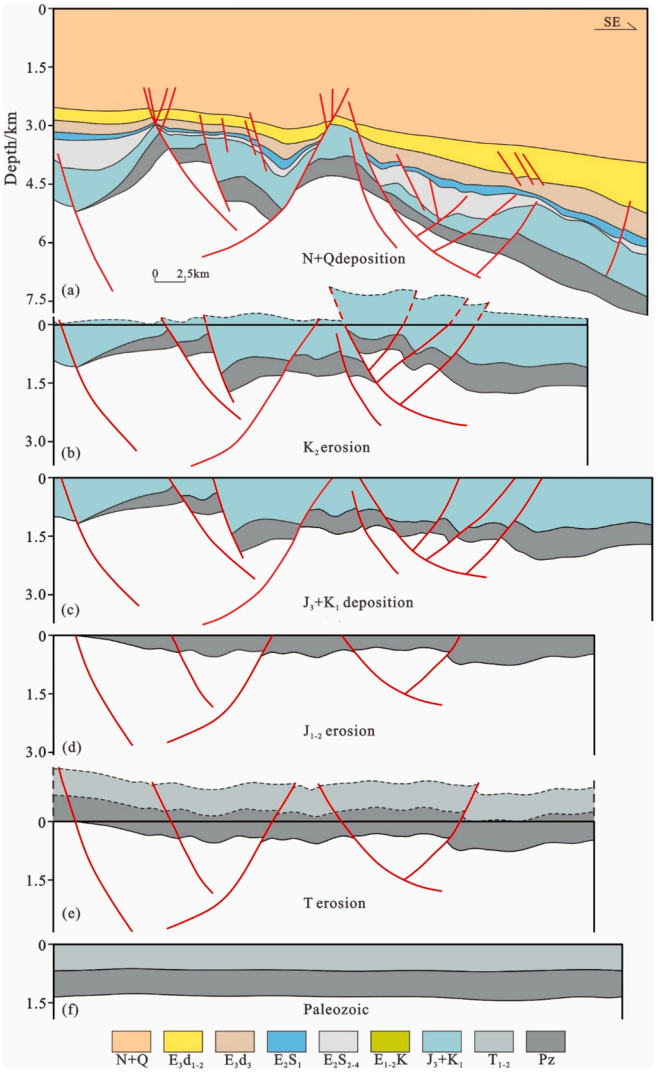

Fig. 14. Balanced restoration of northwest-southeastward profile. Line location is shown in Fig. 1c.

In the northern and central areas, the major NE- and NW-trending faults were continuously active during the Late Cretaceous, and the Mesozoic in the hanging walls was uplifted and eroded, causing the formation of faulted-anticlinal traps. The Late Cretaceous compressional movements induced the formation of numerous structural fractures in the Mesozoic volcanic reservoirs adjacent to the NE- and NW-trending faults. The good source rocks of the Shahejie Formation are directly contacted to the Mesozoic volcanic reservoirs, which benefits the hydrocarbon migration and accumulation (Fig. 16a). In the southern area, the continuous Mesozoic activities of the EW-trending faults induced the entirely erosion of the Mesozoic in local areas of the eastern Shijiutuo uplift (Fig. 16b). The Shijiutuo uplift has experienced multiple compressional activities during the Middle-Late Triassic, Early-Middle Jurassic, and Late Cretaceous, and there are numerous well developed structural fractures in the Archean and Paleozoic reservoirs. Two major boundary faults (F11 and F12 in Fig. 16b) have large fault throws, allowing the source rocks of the Shahejie Formation to be laterally contacted by the Archean reservoirs through the boundary faults, which is helpful for hydrocarbon migration into the Archean faulted horst traps (Fig. 16b). In addition, hydrocarbons can be transport vertically along

Table 1
Calculation results of balanced cross-sections in different periods in the northern Bozhong depression.

Seismic sections in different directions	Structural position of sections	Period	L_0 (km)	L_1 (km)	ΔL (km)	R (%)
NE-SW direction seismic line	Northern and central parts	N + Q	47.81	53.78	5.97	12.48
		K_2	50.05	47.81	−2.24	−4.48
		J_3 + K_1	35.96	50.05	14.09	39.18
		J_{1-2}	36.10	35.96	−0.14	−0.38
		T	37.20	36.10	−1.09	−2.94
NW-SE direction seismic line	Southern part	N + Q	44.08	49.03	4.95	11.23
		K_2	49.41	44.08	−5.33	−10.79
		J_3 + K_1	44.65	49.41	4.76	10.65
		J_{1-2}	44.66	44.65	−0.003	−0.01
		T	46.87	44.66	−2.21	−4.71

Note: L_0-original horizontal length; L_1-horizontal length after deformation; ΔL-change of horizontal length, if it is a positive value, it indicates stretching process, otherwise, it indicates squeezing process; R-ratio of ΔL and L_0, if it is a positive value, it indicates stretching rate, otherwise, it indicates shortening rate.

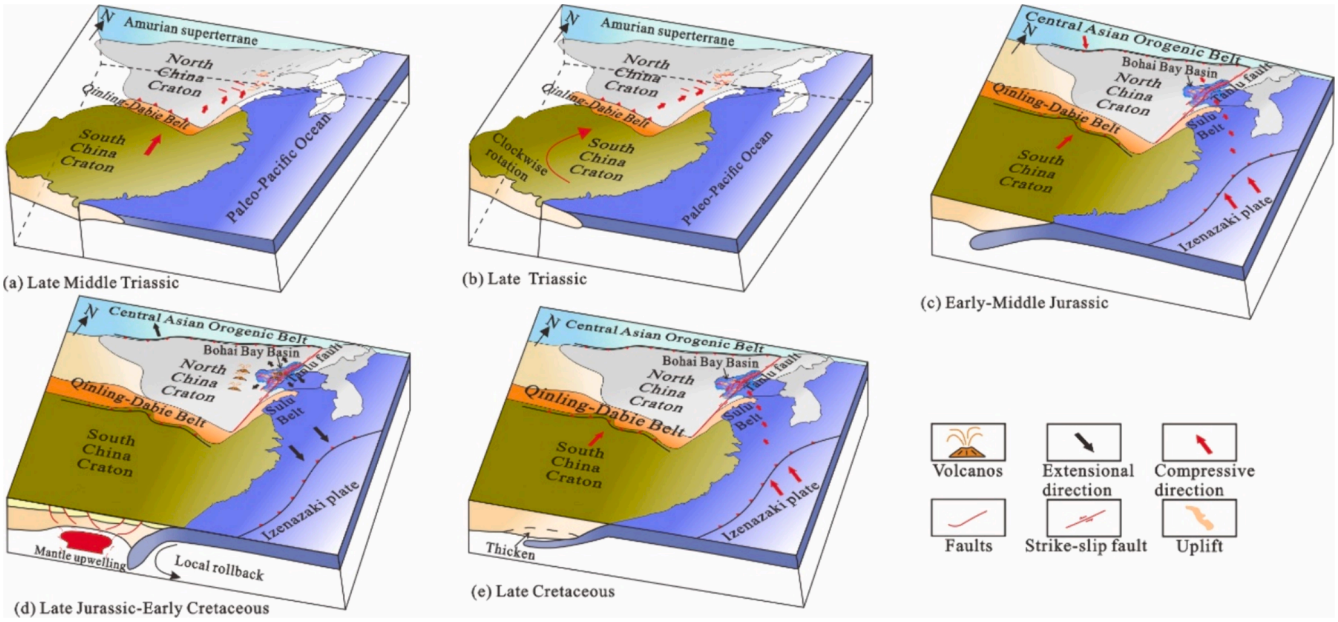

Fig. 15. Geodynamic models showing the Mesozoic evolution of North China Craton. (a) Late Middle Triassic, (b) Late Triassic, (c) Early- Middle Jurassic, (d) Late Jurassic-Early Cretaceous, and (e) Late Cretaceous.

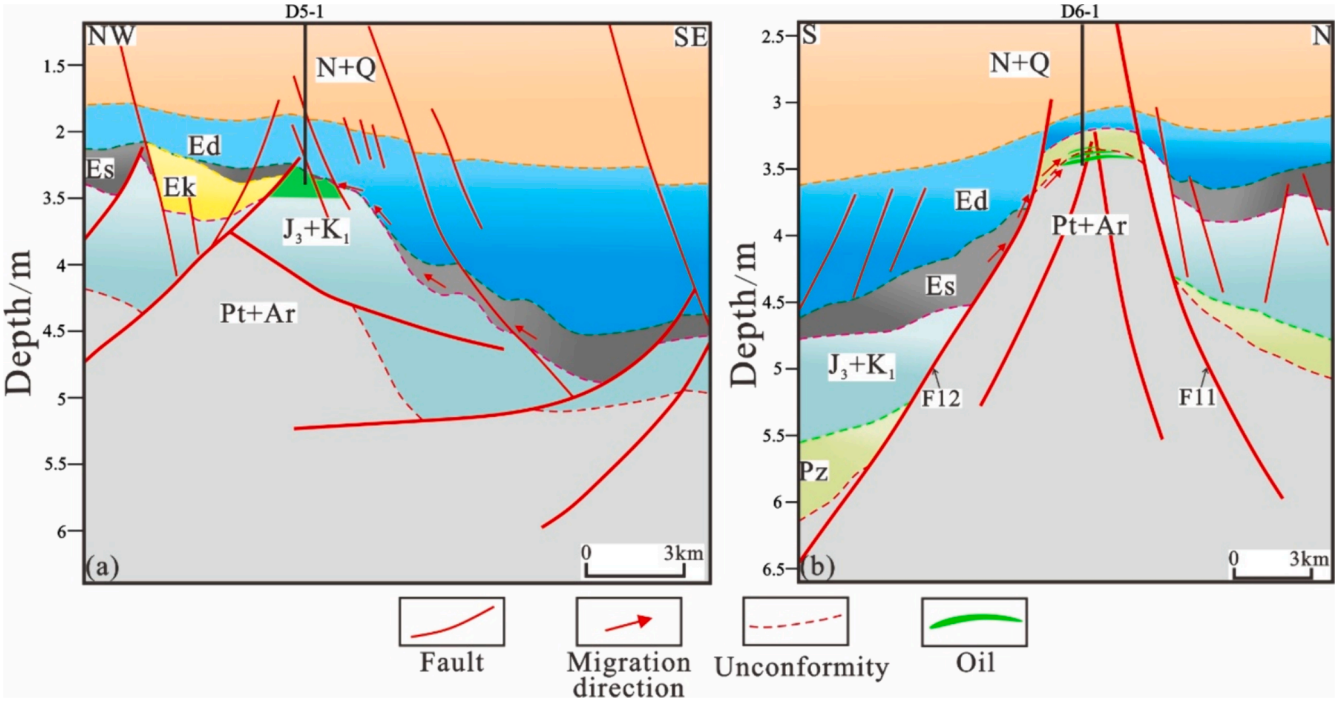

Fig. 16. Two examples of oil pools in buried hills in northern Bozhong depression.

the boundary faults, and then laterally migrate along the unconformity and into the Paleozoic faulted horst traps (Fig. 16b).

6. Conclusion

The complex Mesozoic structural styles of the northern Bozhong depression include compression, strike-slip, and extension structures, which predominantly trend in the near E-W, NW, and NE-NNE. Following the collision and subduction of peripheral plates, the northern Bozhong depression has experienced five stages of deformation during the Mesozoic. At the end of the Middle Triassic, the S-N compressional stress, from the subduction of the South China plate towards the North China plate, induced the formation of near E-W folds and reverse faults in the southern area. Response to the NE-SW tectonic compression during the Late Triassic scissors-type closure processes of the South China and the North China plates, NW-trending folds and reverse faults were formed in the southern and central areas, which were superimposed on the early near E-W structures. In the Early-Middle Jurassic, the high-speed subduction of the Izanagi plate towards the North China plate resulted in the NW-SE compression stress, and the NE-trending transpressional faults were formed in the northern study area. Subsequently, the Late Jurassic-Early Cretaceous thinning of the

lithosphere of the North China Craton induced the NW-SE stretching of the Bohai Bay Basin, giving rise to the formation of a series of the EW-, NW-, and NE-trending fault basins. As a result of the NW-SE compression stress, the study area was wholly folded and uplifted in the Late Cretaceous. The Mesozoic tectonic activities of multiple phases are helpful for the formation of structural traps and fractures, as well as hydrocarbon migration in buried hills of the northern Bozhong depression.

CRediT authorship contribution statement

Fan Yang: Writing – review & editing, Writing – original draft, Validation, Software, Methodology, Investigation. **Yixin Yu:** Writing – review & editing, Supervision, Resources, Project administration, Data curation. **Xintao Zhang:** Visualization, Project administration, Data curation. **Yuhang Chen:** Visualization, Software, Investigation. **Yongjun Liu:** Validation, Project administration, Data curation. **Zhen Zhang:** Validation, Investigation, Data curation. **Peng Qi:** Validation, Data curation. **Yuemeng Niu:** Writing – review & editing, Visualization, Validation.

Declaration of competing interest

The authors declare that they have no known competing financial interests or personal relationships that could have appeared to influence the work reported in this paper.

Data availability

Data will be made available on request.

Acknowledgements

This study was supported by the National Natural Science Foundation of China (Grant No. 42072149) and the Scientific Research Project of CNOOC Limited (CCL2021RCPS0169KQN). The Tianjin Oil Company of CNOOC provided the original 3D seismic survey and the drilling data. The manuscript benefited from constructive reviews by anonymous reviewers and editors.

References

Cheng, Y.J., Wu, Z.P., Lu, S.N., Li, X., Lin, C.Y., Huang, Z.H., Su, W., Jiang, C., Wang, S. Y., 2018. Mesozoic to Cenozoic tectonic transition process in Zhanhua sag, Bohai Bay Basin, east China. Tectonophysics 730, 11–28.

Deng, J.F., Su, S.G., Niu, Y.L., Liu, C., Zhao, G.C., Zhao, X.G., Zhou, S., Wu, Z., 2007. A possible model for the lithospheric thinning of North China Craton: evidence from the Yanshanian (Jura-Cretaceous) magmatism and tectonism. Lithos 96 (2), 22–35.

Dmitrienko, L.V., Wang, P.C., Li, S.Z., Cao, X.Z., Somerville, I., Zhou, Z.Z., Hu, M.Y., Suo, Y.H., Guo, L.L., Wang, Y.M., Li, X.Y., Liu, S.Y., Zhu, J.J., 2018. Meso-Cenozoic evolution of earth surface system under the East Asian tectonic superconvergence. Acta Geol. Sin.-Engl. Ed. 92 (2), 814–849.

Dong, Y.P., Zhang, G.W., Neubauer, F., Liu, X.M., Genser, J., Hauzenberger, C., 2011. Tectonic evolution of the Qinling orogen, China: review and synthesis. J. Asian Earth Sci. 41 (3), 213–237.

Dong, Y.P., Yang, Z., Liu, X.M., Sun, S.S., Li, W., Cheng, B., Zhang, F.F., Zhang, X.N., He, D.F., Zhang, G.W., 2016. Mesozoic intracontinental orogeny in the Qinling Mountains, central China. Gondw. Res. 30, 144–158.

Feng, D.X., Ye, F., 2018. Structure kinematics of a transtensional basin: an example from the Linnan Subsag, Bohai Bay Basin, eastern China. Geosci. Front. 9 (3), 917–929.

Fu, C., Li, S.L., Li, S.L., Xu, J.Y., 2022. Tectonostratigraphic evolution of a rift basin and corresponding source-to-sink systems: implications for the western Bohai Bay Basin. North China. Mar. Pet. Geol. 139, 105587.

Gao, S., Rudnick, R.L., Carlson, R.W., McDonough, W.F., Liu, Y., 2002. Re-Os evidence for replacement of ancient mantle lithosphere beneath the North China craton. Earth Planet. Sci. Lett. 198 (3–4), 307–322.

Ge, X.H., Liu, J.L., Ren, S.M., Yuan, S.H., 2014. The formation and evolution of the Mesozoic-Cenozoic continental tectonics in Eastern China. Geol. China 41 (1), 19–38. In Chinese.

Gibbs, A.D., 1983. Balanced cross-section construction from seismic sections in areas of extensional tectonics. J. Struct. Geol. 5 (2), 153–160.

Hacker, B.R., Ratschbacher, L., Webb, L., Ireland, T., Walker, D., Dong, S.H., 1998. U/Pb zircon ages constrain the architecture of the ultrahigh-pressure Qinling-Dabie Orogen. China. Earth Planet. Sci. Lett. 161 (1–4), 215–230.

Hsiao, L.Y., Graham, S.A., Tilander, N., 2004. Seismic reflection imaging of a major strike-slip fault zone in a rift system: paleogene structure and evolution of the Tan-Lu fault system, Liaodong Bay, Bohai, offshore China. AAPG Bull. 88 (1), 71–97.

Jiang, Y.L., Liu, H., Song, G., Wang, Y.S., Liu, J.D., Zhao, K., Lyu, X.Y., 2017. Differential hydrocarbon enrichment and its Main controlling factors in depressions of the Bohai Bay Basin. Acta Geol. Sin.-Engl. Ed. 91 (5), 1855–1872.

Ju, Y.W., Yu, K., Wang, G.Z., Li, W.Y., Zhang, K.J., Li, S.H., Guo, L.L., Sun, Y., Feng, H., Qiao, P., Ali, R., 2021. Coupling response of the Meso-Cenozoic differential evolution of the North China Craton to lithospheric structural transformation. Earth Sci. Rev. 223, 103859.

Li, S.Z., Kusky, T.M., Liu, X., Zhang, G.W., Zhao, G.C., Wang, L., Wang, Y., 2009a. Two-stage collision-related extrusion of the western Dabie HP–UHP metamorphic terranes, central China: evidence from quartz c-axis fabrics and structures. Gondw. Res. 16 (2), 294–309.

Li, S.Z., Kusky, T.M., Zhao, G.C., Liu, X.C., Wang, L., Kopp, H., Hoernle, K., Zhang, G.W., Dai, L., 2011. Thermochronological constraints on two-stage extrusion of HP/UHP terranes in the Dabie-Sulu orogen, east-central China. Tectonophysics 504 (1–4), 25–42.

Li, S.Z., Guo, L.L., Xu, L.Q., Somerville, I.D., Cao, X.Z., Yu, S., Wang, P.C., Suo, Y.H., Liu, X., Zhao, S., 2015. Coupling and transition of Meso-Cenozoic intracontinental deformation between the Taihang and Qinling Mountains. J. Asian Earth Sci. 114, 188–202.

Li, X.Y., Li, S.Z., Suo, Y.H., Somerville, I.D., Huang, F., Liu, X., Wang, P.C., Han, Z.X., Jin, L.J., 2018b. Early Cretaceous diabases, lamprophyres and andesites-dacites in western Shandong, North China Craton: Implications for local delamination and Paleo-Pacific slab rollback. J. Asian Earth Sci. 160, 426–444.

Li, S.R., Santosh, M., 2014. Metallogeny and craton destruction: records from the North China Craton. Ore Geol. Rev. 56, 376–414.

Li, S.Z., Zhang, G.W., Li, Y.L., Yang, Y.C., 2000. Discovery of granulite in the Mianxian-Lueyang suture zone, Mianxian area and its tectonic significance. Acta Petrol. Sin. 16 (2), 220–226.

Li, S.Z., Liu, X., Suo, Y.H., Liu, L.P., Qian, C.C., Liu, G.W., Zhang, G.W., Zhao, G.C., 2009b. Triassic folding and thrusting in the Eastern Block of the North China Craton and the Dabie-Sulu orogen and its geodynamic. Acta Petrol. Sin. 25 (9), 2031–2049.

Li, S.Z., Zhao, G.C., Dai, L.M., Liu, X., Zhou, L.H., Santosh, M., Suo, Y.H., 2012. Mesozoic basins in eastern China and their bearing on the deconstruction of the North China Craton. J. Asian Earth Sci. 47, 64–79.

Li, S.Z., Suo, Y.H., Santosh, M., Dai, L.M., Liu, X., Yu, S.J., Zhao, S.J., Jin, C., 2013. Mesozoic to Cenozoic intracontinental deformation and dynamics of the North China Craton. Geol. J. 48 (5), 543–560.

Li, S.Z., Suo, Y.H., Li, X.Y., Zhou, J., Santosh, M., Wang, P.C., Wang, G.Z., Guo, L.L., Yu, S.Y., Lan, H.Y., Dai, L.M., Zhou, Z.Z., Cao, X.Z., Zhu, J.J., Liu, B., Jiang, S.H., Wang, G., Zhang, G.W., 2019. Mesozoic tectono-magmatic response in the East Asian ocean-continent connection zone to subduction of the Paleo-Pacific Plate. Earth Sci. Rev. 192, 91–137.

Li, W., Zhang, F., Zhang, Y., Fu, L., Li, H., 2021. Characteristics and formation mechanisms of Mesozoic compressional structures in the Huanghua Depression, Bohai Bay Basin. China. Aust. J. Earth Sci. 68 (5), 746–761.

Li, S.Z., Zhao, S.J., Liu, X., Cao, H.H., Yu, S., Li, X.Y., Somerville, I., Yu, S.Y., Suo, Y.H., 2018a. Closure of the Proto-Tethys Ocean and Early Paleozoic amalgamation of microcontinental blocks in East Asia. Earth Sci. Rev. 186, 37–75.

Liu, S., Qian, T., Li, W.P., Dou, G.X., Wu, P., 2015. Oblique closure of the northeastern Paleo-Tethys in central China. Tectonics 34 (3), 413–434.

Liu, S., Gurnis, M., Ma, P., Zhang, B., 2017. Reconstruction of northeast Asian deformation integrated with western Pacific plate subduction since 200 Ma. Earth Sci. Rev. 175, 114–142.

Liu, Y.M., Liu, L.J., Wu, Z.P., Li, W., Hao, X., 2022. New insight into East Asian tectonism since the late Mesozoic inferred from erratic inversions of NW-trending faulting within the Bohai Bay Basin. Gondw. Res. 102, 17–30.

Liu, S.F., Zhang, J.F., Hong, S.Y., Bradley, D.R., 2007. Early Mesozoic basin development and its response to thrusting in the Yanshan fold-and-thrust belt. China. Int. Geol. Rev. 49 (11), 1025–1049.

Liu, S.F., Su, S., Zhang, G.W., 2013. Early Mesozoic basin development in North China: indications of cratonic deformation. J. Asian Earth Sci. 62, 221–236.

Lu, L.L., Jiang, S.H., Li, S.Z., Wang, P.C., Jiang, Y., Wang, G., Zhang, W., Suo, Y.H., Santosh, M., 2022. Evolution of Meso-Cenozoic subduction zones in the ocean-continent connection zone of the eastern South China Block: insights from gravity and magnetic anomalies. Gondw. Res. 102, 151–166.

Meng, Q.R., Wu, G.L., Fan, L.G., Wei, H.H., 2019. Tectonic evolution of early Mesozoic sedimentary basins in the North China block. Earth Sci. Rev. 190, 416–438.

Qi, J.F., Yu, F.S., Lu, K.Z., 2003. Conspectus on Mesozoic basins in Bohai Bay province. Earth Sci. Front. 10, 199–206.

Su, J.B., Zhu, W.B., Lu, H.F., Xu, M.J., Yang, W., Zhang, Z., 2009. Geometry styles and quantification of inversion structures in the Jiyang depression, Bohai Bay Basin, eastern China. Mar. Pet. Geol. 26 (1), 25–38.

Suo, Y.H., Li, S.Z., Cao, X.Z., Wang, X.Y., Somerville, I., Wang, G.Z., Wang, P.C., Liu, B., 2020. Mesozoic-Cenozoic basin inversion and geodynamics in East China: a review. Earth Sci. Rev. 210, 103357.

Wang, G.Z., Li, S.Z., Li, X.Y., Zhao, W.Z., Zhao, S.J., Suo, Y.H., Liu, X.G., Somerville, I., Zhou, J., Wang, Z.C., 2019. Destruction effect on Meso-Neoproterozoic oil-gas traps derived from Meso-Cenozoic deformation in the North China Craton. Precambr. Res. 333, 105427.

Wang, Q., Sun, Y.H., Zhang, W.F., Wang, Y.G., Cao, L.Z., Li, X.W., 2022. Structural characteristics and mechanism of the Hengshui accommodation zone in the southern Jizhong subbasin, Bohai Bay Basin. China. Mar. Pet. Geol. 138, 105558.

Wang, Y., Zhou, L.Y., Liu, S.F., Li, J.Y., Yang, T.N., 2018. Post-cratonization deformation processes and tectonic evolution of the North China Craton. Earth Sci. Rev. 177, 320–365.
Wang, Y., Xu, C.Q., Guo, L.L., Liu, Y.J., Wang, G.Z., Liu, B., Li, S.Z., Guan, X.Q., Jiang, L. W., Chen, Z.X., Li, F.K., Zhou, Q.J., Yuan, Q.L., 2021. Structural analysis of Shijiutuo east 428 buried hill in Bohai Bay Basin: implications on destruction of the North China Craton. Geotecton. Metallog. 45 (1), 219–228. In Chinese.
Wu, Z.P., Hou, X.B., Li, W., 2007. Discussion on Mesozoic basin patterns and evolution in the eastern North China Block. Geotecton. Metallog. 31 (4), 385–399. In Chinese.
Wu, F.Y., Yang, J.H., Xu, Y.G., Wilde, S.A., Walker, R.J., 2019. Destruction of the North China craton in the Mesozoic. Annu. Rev. Earth Planet. Sci. 47, 173–195.
Xu, Y.G., 2007. Diachronous lithospheric thinning of the North China Craton and formation of the Daxin'anling–Taihangshan gravity lineament. Lithos 96 (1–2), 281–298.
Xu, Z., Zhao, Z.F., Zheng, Y.F., 2012. Slab–mantle interaction for thinning of cratonic lithospheric mantle in North China: geochemical evidence from Cenozoic continental basalts in central Shandong. Lithos 146, 202–217.
Yang, F., Santosh, M., Kim, S.W., 2018. Mesozoic magmatism in the eastern North China Craton: insights on tectonic cycles associated with progressive craton destruction. Gondw. Res. 60, 153–178.
Yang, F., Chen, Y.H., Zhang, X.T., Yu, Y.X., Liu, Y.J., Zhang, Z., Niu, Y.M., 2022a. Characteristics of the pre-Paleogene faults and their influences on buried-hill strata at the south pitching end of the Liaoxi low uplift. Bohai Sea. China Offshore Oil Gas. 34 (6), 14–23. In Chinese.
Yang, C.S., Li, S.Z., Li, G., Yang, C.Q., Yang, Y.Q., Dai, L.M., Suo, Y.H., Jiang, Y.B., 2016. Tectonic units and proto-basin of the East China Sea Shelf Basin: correlation to Mesozoic subduction of the Palaeo-Pacific Plate. Geol. J. 51, 149–161.
Yang, F., Song, C.Z., Ren, S.L., Ji, M.H., 2022b. The mesozoic tectonic transition from compression to extension in the South China block: insight from structural deformation of the Lushan Massif. SE China. Minerals 12 (12), 1531.
Yin, A., Nie, S., 1993. An indentation model for the North and South China collision and the development of the Tan-Lu and Honam fault systems, eastern Asia. Tectonics 12 (4), 801–813.
Yu, Y.X., Zhou, X.H., Tang, L.J., Peng, W.X., Lu, D.Y., Li, W.G., 2009. Salt structures in the Laizhouwan depression, offshore Bohai Bay Basin, eastern China: new insights from 3D seismic data. Mar. Pet. Geol. 26 (8), 1600–1607.
Yu, Y.X., Zhou, X.H., Xu, C.G., Wu, K., Lv, D.Y., Liu, Y.B., Zhou, X., 2020. Architecture and evolution of the Cenozoic offshore Bohai Bay Basin, eastern China. J. Asian Earth Sci. 192, 104272.
Zhang, J.D., Hao, T.Y., Dong, S.W., Chen, X.H., Cui, J.J., Yang, X.Y., Liu, C.Z., Li, T.J., Xu, Y., Huang, S., Re, F.L., 2015. The structural and tectonic relationships of the major fault systems of the Tan-Lu fault zone, with a focus on the segments within the North China region. J. Asian Earth Sci. 110, 85–100.
Zhang, Z., Zhang, X.T., Xu, C.Q., Wu, Q.X., Li, L., 2019. Tectonic evolution and its controlling on hydrocarbon accumulation of 428 Buried Hill in Bohai Sea. J. Northeast. Pet. Univ. 43 (4), 69–77. In Chinese.
Zhang, S., Zhu, G., Liu, C., Li, Y.J., Su, N., Xiao, S.Y., Gu, C.C., 2018. Strike-slip motion within the Yalu River Fault Zone, NE Asia: the development of a shear continental margin. Tectonics 37 (6), 1771–1796.
Zhao, Y., Yang, Z.Y., Ma, X.H., 1994. Geotectonic transition from paleoasian system and paleotethyan system to paleopacific active continental margin in eastern Asia. Chin. J. Geol. 29 (2), 105–119. In Chinese.
Zheng, J.P., Dai, H.K., 2018. Subduction and retreating of the western Pacific plate resulted in lithospheric mantle replacement and coupled basin-mountain respond in the North China Craton. Sci. China Earth Sci. 61, 406–424.
Zhou, L.H., Fu, L.X., Lou, D., Lu, Y., Feng, J.Y., Zhou, S.H., Santosh, M., Li, S., 2012. Structural anatomy and dynamics of evolution of the Qikou Sag, Bohai Bay Basin: implications for the destruction of North China craton. J. Asian Earth Sci. 47, 94–106.
Zhou, Z.Z., Li, S.Z., Li, X.Y., Guo, L.L., Liu, X.G., Guo, R.H., Somerville, I., 2017. Triassic orocline in East Asia: insights from a transition from passive margin to foreland basin in eastern North China Block. Geol. J. 52, 59–69.
Zhu, R., Chen, L., Wu, F., Liu, J., 2011. Timing, scale and mechanism of the destruction of the North China Craton. Sci. China Earth Sci. 54 (6), 789–797.
Zhu, G., Chen, Y., Jiang, D., Lin, S.Z., 2015a. Rapid change from compression to extension in the North China Craton during the Early Cretaceous: evidence from the Yunmengshan metamorphic core complex. Tectonophysics 656, 91–110.
Zhu, R., Fan, H., Li, J., Meng, Q., Li, S., Zeng, Q., 2015b. Decratonic Gold Deposits. Sci. China-Earth Sci. 58, 1523–1537.
Zhu, J.C., Feng, Y.L., Meng, Q.R., Wu, F.C., Li, H., Liu, H.T., Zhang, F.P., Wang, T.Y., Wu, G.L., Zou, C.N., Zhu, R.X., 2019. Late Mesozoic tectonostratigraphic division and correlation of the Bohai Bay Basin: implications for the Yanshanian Orogeny. Sci. China Earth Sci. 62, 1783–1804.
Zhu, G., Jiang, D.Z., Zhang, B.L., Chen, Y., 2012. Destruction of the eastern North China Craton in a backarc setting: evidence from crustal deformation kinematics. Gondw. Res. 22 (1), 86–103.
Zhu, G., Liu, C., Gu, C.C., Zhang, S., Li, Y.J., Su, N., Xiao, S., 2018. Oceanic plate subduction history in the western Pacific Ocean: constraint from late Mesozoic evolution of the Tan-Lu Fault Zone. Sci. China-Earth Sci. 61, 386–405.
Zhu, Y.B., Liu, S.F., Zhang, B., Gurnis, M., Ma, P.F., 2021. Reconstruction of the Cenozoic deformation of the Bohai Bay Basin. North China. Basin Res. 33 (1), 364–381.
Zhu, R.X., Xu, Y.G., 2019. The subduction of the west Pacific plate and the destruction of the North China Craton. Sci. China Earth Sci. 62, 1340–1350.